

Numerical Simulation of Sea Bed Response under Waves with Coupled Solver of Biot Consolidation Equations and Free Surface Water Flow

Xiaofeng Liu and Marcelo H. García
Ven Te Chow Hydrosystems Laboratory,
Department of Civil and Environmental Engineering,
University of Illinois at Urbana and Champaign,
Urbana, IL, USA

ABSTRACT

A 3D numerical model for the sea bed response under free surface water waves is constructed. Free surface is modeled by Volume of Fluid (VOF) method and water wave is generated by numerical wave maker boundary condition. An iterative numerical scheme is proposed to solve Biot consolidation equation using finite volume method (FVM). The coupling between water wave and sea bed is through pressure and stress condition on common boundaries. Numerical test shows good agreement with analytical solution. 3D application of sea bed response under waves with the presence of object is also carried out to investigate the liquefaction potential.

KEY WORDS: Sea bed; wave; Biot consolidation; free surface; fluid structure interaction.

INTRODUCTION

The interest in wave-seabed-structure interaction is growing because it is important for geotechnical engineers to design offshore engineering projects (such as pipe lines, piles and break waters). Also sinking/floating of objects on the sea bed (such as wrecked ships, mines) is closely related to the sea bed response under waves. Many experiments (Sakai et al, 1994; Sumer et al, 1999) and numerical simulations (Magda, 1996; Jeng and Lin, 1999; Gao et al, 2003) have been done to try to understand this complicated process. There are also many analytical models which describe the sea bed response and give fairly good results (Yamamoto, 1977; Mei and Foda, 1981; Jeng and Hsu, 1996; Yuh and Ishida, 2002).

Many numerical models have been developed to solve sea bed response under wave. But most of the models just assume the wave pressure on the water-bed interface using wave theory. This is applicable as a first order approximation for many cases if there is only water wave and sea bed interaction. But for the case when there is extra object in the system (such as pile, semi-buried foundation, etc.), the water flow around the object will be highly three dimensional and is not easy to get an analytical solution from wave theory. Multi-physics numerical models

have been widely used to solve coupled system. The approach in these models is to solve different governing equations on different domains and couple the system through common boundary or other ways. This is also the approach used in this paper. 3D computational fluid dynamics (CFD) models is used to predict the free surface wave field and the results can be used as boundary condition for the sea bed governing equations.

Traditionally, the Biot consolidation equations used in this paper to describe the sea bed response are solved via finite element method (FEM). FEM is the most widely used method in stress analysis. But FVM is gaining popularity in this area because it is good at treating complicated, coupled and non-linear differential equations (Jasak and Weller, 2000). Application of FVM in stress analysis can be found, among many others, in Demidžić et al (1994) and Demidžić et al (1997). An iterative scheme for the Biot consolidation equation using FVM is proposed in this paper. Momentary liquefaction potential due to waves is assessed based on the numerical result of consolidation.

The structure of this paper is as following. Governing equations of the coupled system are described first. Then the numerical schemes used in this paper are discussed. Numerical verification and application of the current model are provided. Discussion and conclusion are at the end of the paper.

GOVERNING EQUATIONS

Fig. 1 shows a typical experiment setup for the sea bed response under waves. Governing equations in different parts of the domain (sea bed domain and fluid domain) are listed below. The fluid flow in is governed by Navier-Stokes equations with $k-\epsilon$ turbulence model. The sea bed response is governed by Biot consolidation equations.

Navier-Stokes Equations

The governing equations for the wave part are the Navier-Stokes equations:

$$\nabla \cdot \mathbf{u} = 0 \quad (1)$$

$$\frac{\partial \rho \mathbf{u}}{\partial t} + \nabla \cdot (\rho \mathbf{u} \mathbf{u}) - \nabla \cdot (\mu \mathbf{S}) = -\nabla p + \rho \mathbf{g} \quad (2)$$

where \mathbf{u} is the velocity vector, p is pressure

\mathbf{S} is the strain rate tensor defined by $\mathbf{S} = \frac{1}{2} [\nabla \mathbf{u} + (\nabla \mathbf{u})^T]$. The density ρ and viscosity μ in the domain are given by

$$\rho = \alpha \rho_1 + (1 - \alpha) \rho_2 \quad (3)$$

$$\mu = \alpha \mu_1 + (1 - \alpha) \mu_2 \quad (4)$$

where α is the volume fraction function for the two fluids defined by

$$\alpha = \begin{cases} 0 & \text{volume occupied by air} \\ 1 & \text{volume occupied by water} \end{cases} \quad (5)$$

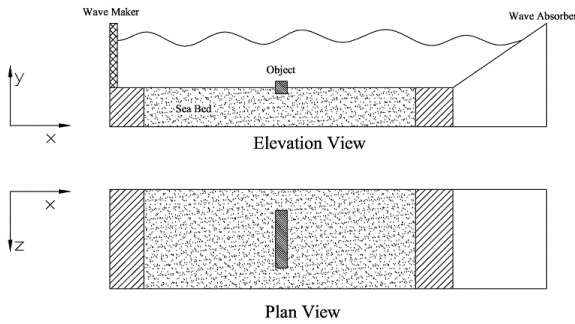


Fig. 1 Typical experimental setup for sea bed response under waves

Volume fraction α is transported by the fluid velocity field. The equation for the volume fraction scalar α is

$$\frac{\partial \alpha}{\partial t} + \nabla \cdot (\mathbf{u} \alpha) = 0 \quad (6)$$

Numerical diffusion will spread out the sharp interface between water and air. A compressive interface capturing scheme is used to sharpen the interface. The details of the present free surface modeling can be found in Ubbink and Issa (1999).

The turbulence flow field is modeled by $k - \varepsilon$ model (Lauder and Spalding, 1973):

$$\mu_t = C_\mu \rho \frac{k^2}{\varepsilon} \quad (7)$$

$$\frac{\partial k}{\partial t} + \nabla \cdot (\mathbf{u} k) = \frac{1}{\rho} \nabla \cdot \left(\frac{\mu_t}{\sigma_k} \nabla k \right) + 2 \frac{\mu_t}{\rho} |\nabla \mathbf{u}|^2 - \varepsilon \quad (8)$$

$$\frac{\partial \varepsilon}{\partial t} + \nabla \cdot (\mathbf{u} \varepsilon) = \frac{1}{\rho} \nabla \cdot \left(\frac{\mu_t}{\sigma_\varepsilon} \nabla \varepsilon \right) + 2 \frac{C_1 \mu_t}{\rho} |\nabla \mathbf{u}|^2 \frac{\varepsilon}{k} - C_2 \frac{\varepsilon^2}{k} \quad (9)$$

where μ_t is the eddy viscosity, k is turbulence kinetic energy and ε is turbulence energy dissipation rate. The constants C_μ , C_1 , C_2 , σ_k , σ_ε take the values of 0.09, 1.44, 1.92, 1.0, 1.3 respectively.

Biot Consolidation Equations

Governing equations for the poro-elastic sea bed two phase media is the Biot consolidation equation (Biot, 1941):

$$G \nabla^2 \mathbf{v} + \frac{G}{1 - 2\nu} \nabla (\nabla \cdot \mathbf{v}) = \nabla p \quad (10)$$

$$\frac{k}{\gamma} \nabla^2 p = \frac{n}{K} \frac{\partial p}{\partial t} + \frac{\partial}{\partial t} (\nabla \cdot \mathbf{v}) \quad (11)$$

Eq. 10 is the force balance equation of the bed soil and Eq. 11 is the storage equation which describes the mass balance of the pore water. Here p is the pore water pressure, \mathbf{v} is the displacement vector of soil skeleton. G is the shear modulus of soil, ν is the Poisson ratio of the soil, K is the coefficient of the isotropic permeability, γ is the specific weight of water, β is the compressibility of pore water, n is soil porosity. These equations assume that the hydraulic permeability is isotropic and the stress-strain relationship is linear. Strain tensor ε is defined in terms of the displacement vector \mathbf{v} as

$$\varepsilon = \frac{1}{2} [\nabla \mathbf{v} + (\nabla \mathbf{v})^T] \quad (12)$$

the stress tensor $\boldsymbol{\sigma}$ is related to the strain rate ε via

$$\boldsymbol{\sigma} = \boldsymbol{\sigma}' - p \mathbf{I} = 2G \varepsilon + \left[2G \frac{\nu}{1 - 2\nu} \text{tr}(\varepsilon) - p \right] \mathbf{I} \quad (13)$$

where \mathbf{I} is the unit diagonal tensor. $\text{tr}(\varepsilon)$ is the trace of the tensor ε . Eq. 13 says that the stress in soil is constituted by two parts: the effective stress $\boldsymbol{\sigma}'$ supported by soil skeleton and pore water pressure p . Plain strain is also assumed here.

NUMERICAL SCHEMES AND PROCEDURE

The code used in this research is the open source numerical library OpenFOAM (2005). It's freely available through internet. OpenFOAM is primarily designed for problems in continuum mechanics. It uses the tensorial approach and object oriented techniques (Weller et al, 1998). OpenFOAM provides a fundamental platform to write new solvers for different problems as long as the problem can be written in tensorial partial differential equation forms. In this research, the flow field is solved by the adaptation of the original turbulence solver for incompressible fluid in the code. The consolidation equation solver is newly added. The core of this code is the finite volume discretization of the governing equations. Almost all kinds of differential operators possible in a partial differential equation, such as temporal derivative, divergence, laplacian operator, curl, etc. can be discretized in the code. Next several sections briefly introduce the numerical schemes used in the coupled solvers.

Numerical Scheme for Fluid Wave Part

The numerical solution for Navier-Stokes equation of incompressible fluid flow imposes two main problems (Jasak, 1996): the nonlinearity of momentum equation and the pressure-velocity coupling. For the first problem, two common methods can be used to deal with it. The first is to solve nonlinear algebra systems after the discretization. This will need a lot of computational effort. The other is to linearize the convection term in the momentum equation by using the fluid velocity in old time steps which satisfies the divergence-free condition. The latter method is used in this research. For pressure-velocity coupling, many schemes exist, such as SIMPLE (Patankar, 1981) and PISO (Issa, 1986). PISO scheme is used in this code. For the $k-\varepsilon$ turbulence model equations, although these equations are coupled together, they are solved by segregated approach, which means they are solved one at a time. This is also the usual approach used in most CFD codes.

There are two grids in the computational domain. One is for the fluid and the other is for the sea bed. Since no governing differential equation is specified on the object, no grid is needed for it. In some cases such as ocean pipe line analysis, the deformation of those pipes under wave is important and the grid for the pipe is needed (Magda, 1996). Fig. 1 shows how the two grids (wave tank and sea bed) are used to do coupling computations. Information is transferred between fluid grid and sea bed grid via the common boundary, i.e. sea bottom. The figure also shows the presence of an object.

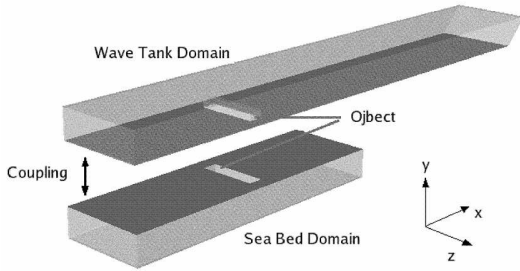


Fig. 2 Coupling Between Fluid Domain and Bed Domain

Numerical Scheme for Sea Bed Part

Finite element method is usually used to solve the Biot equations of soil consolidation (Lewis and Schrefler, 1998) and to do other stress analysis. But finite volume method is becoming popular because of its flexibility to deal with complex domain. In this paper, FVM is used to solve the consolidation equations. Comparing the Biot consolidation equations with the Navier-Stokes equations shows they are very similar. Both equations couple two quantities (pore pressure and displacement for consolidation, pressure and velocity for fluid) and both equations describe the mass balance and force balance. Inspired by these similarities, a new scheme is proposed to solve consolidation equations on an iterative basis. This iterative procedure is similar to the SIMPLE and PISO schemes for Navier-Stokes equations. A segregated approach is used to solve the couple consolidation equation which means components of the displacement vector and pore pressure is solved separately. At each time step, storage equation (Eq. 11) is rearranged into implicit and explicit parts and is solved first according to

$$\underbrace{-\frac{n}{K'} \frac{\partial p}{\partial t} + \frac{k}{\gamma} \nabla^2 p}_{\text{implicit}} = \underbrace{\frac{\partial}{\partial t} (\nabla \cdot \mathbf{v})}_{\text{explicit}} \quad (14)$$

where the displacement \mathbf{v} in the explicit part is from previous iteration or initial condition. Then the force balance equation (Eq. 10) is solved. In order to get higher efficiency of the segregated solver and to increase the convergence radius, a decomposition and a rearrangement of Eq. 10 is carried out similar to Jasak and Weller (2000). The terms in the equation are also split into implicit part and explicit part. The aim is to achieve maximum simplicity. Assuming G and μ are constants, using the fact

$$\nabla (\nabla \cdot \mathbf{v}) = \nabla \cdot (\mathbf{I} \nabla \cdot \mathbf{v}) = \nabla \cdot (\mathbf{I} \text{tr} (\nabla \mathbf{v})) \quad (15)$$

the force balance equation can be written as

$$\underbrace{G \nabla^2 \mathbf{v} + \frac{G}{1-2\nu} \nabla^2 \mathbf{v}}_{\text{implicit}} = \nabla p - \nabla \cdot \left(\underbrace{\frac{G}{1-2\nu} \mathbf{I} \text{tr} (\nabla \mathbf{v}) - \frac{G}{1-2\nu} \nabla \mathbf{v}}_{\text{explicit}} \right) \quad (16)$$

Eq. 16 is solved for each component of vector \mathbf{v} and the resulting \mathbf{v} is used to solve storage equation again. This inner coupling is looped until desired convergence tolerance is achieved.

Boundary Conditions

Boundary Conditions for the Fluid Domain

The wave in the physical experiment is usually generated by a piston type wave maker and at the end of the wave tank, there is a wave absorber to eliminate the wave reflection. In numerical simulation, the wave can be generated generally by two approaches: moving mesh (Aliabadi et al, 2003) and wave boundary condition (Mayer et al, 1998). For moving mesh approach, the piston movement is simulated by moving the boundary of the computational domain. For wave boundary condition approach, the mesh is fixed but boundary condition on the piston part is given by wave theory. The second approach is adopted in this paper. A time varying velocity profile is imposed at the piston boundary to generate the waves

$$\mathbf{U}(y) = f_r(t) \left[U_a(y) \sin(\omega t + \theta) \right] \quad (17)$$

where $\mathbf{U}(y)$ is the velocity vector at the wave generator boundary, $U_a(y)$ is the imposed by the type of the piston, ω is the wave frequency, θ is the phase. $f_r(t)$ is the ramp function to start the piston. $f_r(t)$ has the form

$$f_r(t) = \begin{cases} \frac{t}{T} - \frac{1}{\pi} \sin\left(\pi \frac{t}{T}\right) & \text{for } 0 < t < T \\ 1 & \text{for } t > T \end{cases} \quad (18)$$

where T is the wave period.

The wave absorber is simulated using a damping zone (or sponge layer). In this damping zone, extra fluid viscosity is added to the momentum equation to dissipate the fluid dynamic energy. In numerical test cases, in order to eliminate the introduced artificial effect, the damping zone is extended far downstream. That's the reason that the wave tank domain used in this paper will be longer than the sea bed domain. An alternative method by modifying the water depth and fluid velocity in the damping zone can be found in Mayer et al (1998).

At the piston, pressure is set to be zero normal gradient to be consistent with velocity condition. Turbulence quantities such as k and \mathcal{E} are set as zero normal gradient at the piston wall. The top boundary of the fluid domain is atmosphere. The dynamic pressure is set to zero as the outlet and the velocity is set to zero. Other quantities are set to zero normal gradient. At the object's surfaces or flume walls, it is assumed to be hydraulically smooth. No-slip condition is set for velocity with zero normal gradient for pressure. Other quantities such as k and \mathcal{E} are also set as zero normal gradient.

Boundary Conditions for the Sea Bed Domain

In this paper, only finite soil depth is considered for the sea bed domain because it's the case for most of the physical experiments. Infinite soil depth case can be achieved by extending the sea bed downward until the numerical result won't change anymore. The boundary conditions for the sea bed domain are very similar to Magda (1996) and Jeng and Lin (1999). At the bottom of the sea bed, zero displacements and zero vertical flow are specified, i.e.

$$\mathbf{v} = 0 \quad (19)$$

$$\frac{\partial p}{\partial \mathbf{n}} = 0 \quad (20)$$

where \mathbf{n} is the surface normal direction vector.

At the top of sea bed (i.e. the common boundary between two domains), the fluid shear stress is neglected since it is small comparing to the normal stress (Sumer and Fredsøe, 2002). The pore water pressure at the sea bed is equal to water wave pressure on the bed. This pressure value comes from the fluid solver. For the displacement on this surface, it's more complicated. Since the pore water pressure is set to be the wave pressure, the effective normal stress σ'_{yy} on this boundary is zero. This gives the boundary condition of Neumann type (traction boundary) for displacement (Demidžić et al, 1994; Jasak and Weller, 2000)

$$\mathbf{n} \cdot \nabla \mathbf{v} = \frac{\mathbf{t} - \mathbf{n} \cdot \left[\mu (\nabla \mathbf{v})^T - (\mu + \lambda) \nabla \mathbf{v} \right] - \lambda \mathbf{n} \cdot \nabla \cdot \mathbf{v}}{2\mu + \lambda} \quad (21)$$

where \mathbf{t} is the traction stress on the bed which is equal to zero for the free bed surface in this case.

On the surfaces of object, it's assumed that no water can flow through. So zero pressure gradient as in Eq. 20 applies. For the displacement on the object, the object sides and bottom are considered separately. For the object sides, it's assumed that the sides are smooth and the soil can slip on the surface. The normal displacement components on the sides are set to zero. For the object bottom, the traction boundary condition

(Eq. 20) is specified. The traction on the bottom is from the simple force balance of the object (see Fig. 3). The forces on the object are flow drag F_{drag} , flow lift F_{lift} , gravity force mg and bottom supporting force. The friction forces on the object sides are neglected. This is reasonable because the sand on the sides of the object can be assumed loosely back filled in experiment. The flow drag and lift are calculated at each time step from the flow solver. So the Neumann type condition in Eq. 21 is applied with traction \mathbf{t} from force balance of the object. This assumption is valid if the object is rigid body and will not move. It will be violated if the object is moving under wave force.

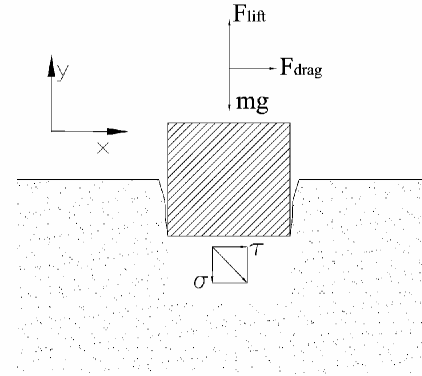


Fig. 3 Force Balance of the Object

Simulation Process

In order to get the effect of waves, base state of pore pressure and displacement without wave is obtained by doing the computation for a period of time with the wave maker shut off. This resembles the fact that in experiment, the bed soil is already in the equilibrium state before the wave maker is started. After that, the wave maker boundary condition is switched on and the wave is generated. Base stable pore pressure and displacement is subtracted from the result to investigate the effect of waves. The main application of current numerical model is the study of liquefaction potential. When the pore water pressure is so excessive that the effective stress in soil is zero or negative, the soil is in the state of liquefaction (Jeng and Hsu, 1996). For a flat bed, the criterion for liquefaction is

$$\frac{p}{\frac{1}{3}(\gamma_s - \gamma_w)(1 + 2K_0)y} \geq 1 \quad (21)$$

where p is excessive pore pressure, γ_s and γ_w are unit weight of soil and water, K_0 is the coefficient of lateral earth pressure at rest which ranges from 0.4 to 1.0. y is the depth of the soil measured downward from the bed. But for complicated computational domain, it's not easy to calculate the effective soil gravity force at each point in the bed. In this paper, the dimensionless excessive pore water pressure (non-dimensionalized by $p_0 = \rho g H_0$, where H_0 is the wave height) is used as an indicator for the liquefaction potential. Other parameters and liquefaction criterion based on effective soil stress can also be used.

At each time step, the fluid field is first solved and the pressure on the sea bed is mapped to the bed domain. Based on the pressure from fluid

solver, the Biot consolidation equations are solved. This process continues until wave period averaged pore pressure and displacement reach steady state or the specified computation time is reached.

MODEL VERIFICATION AND APPLICATION

Verification of FVM Solver for Consolidation Equations

In order to verify the Biot equation solver in the numerical model, a test case which is similar to that of Jeng and Lin (1999) is carried out. Fig. 4 is the schematic view of the test case. The details of the test case can be found in the original paper and the analytical solution can be found in Jeng and Hsu (1996). In this test case, uniform sea bed is under the progressive wave. The bed soil depth $h = 1\text{m}$ and the wave pressure amplitude $p_b = 2000\text{N/m}^2$. The wave number $k = \pi$ and wave frequency $\omega = 2\pi$.

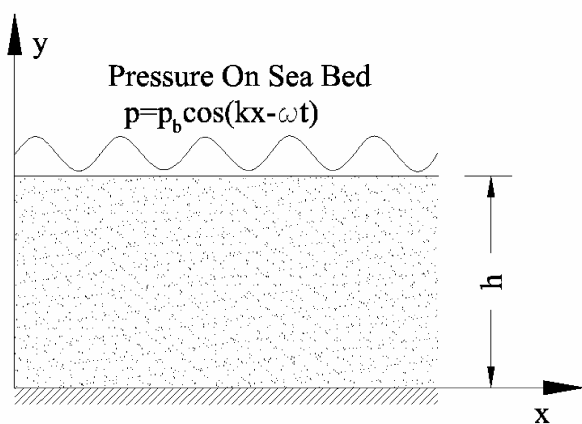


Fig. 4 Numerical Test of Sea Bed Response

The numerical result of excessive pore pressure at each depth of the soil versus $kx - \omega t$ is plotted in Fig. 5. The analytical solution is also plotted. The difference between numerical result and analytical solution is so small that they are almost identical to each other. From the figure, the excessive pore pressure diffuses with the increase of depth which is as expect. For flat bed, top layers of soil are most vulnerable to storm waves and failure of foundation due to liquefaction always happens in these layers.

Fig. 6 shows the numerical results of the test case. Fig. 6(a) shows the pore water pressure and Fig. 6(b) shows the displacement magnitude. From the figures, it's clear that under wave crest the pressure on the bed is increased and the soil is compressed. Under wave trough, it's just the opposite. The displacement vector field in Fig. 7 demonstrates this pattern even more clearly. The geometry in this figure is distorted by 10000 times the displacement to show elastic deformation.

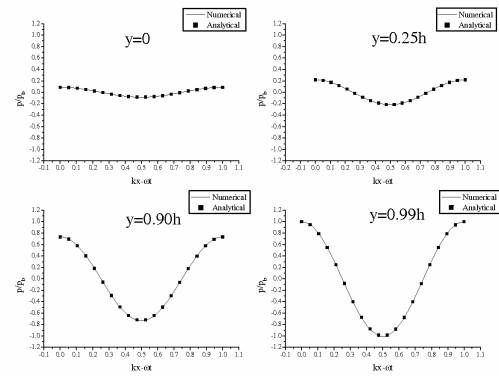


Fig. 5 Pore Pressure Comparison between Numerical and Analytical Solution

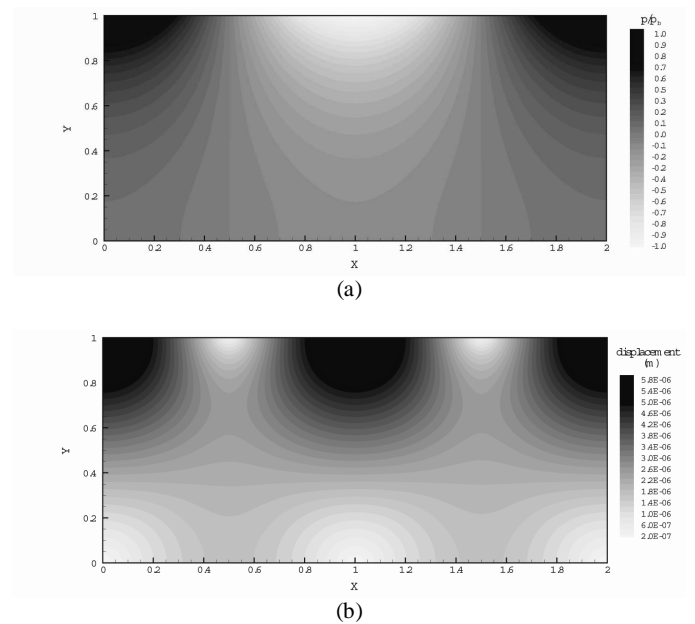


Fig. 6 Displacement of Consolidation Test Case: (a) Pore Pressure (b) Magnitude of Displacement

3D Test Case of Sea Bed Response under Waves with Presence of an Object

In this test case, 3D sea bed response in the numerical wave tank is simulated. The wave tank is 40m long and 3m wide. The water depth in the tank is 1m. An object (which is represented by a box of dimensions $2\text{m} \times 0.5\text{m} \times 0.5\text{m}$ is half buried in the sand (see Fig. 1). The presence of the object will change the wave flow field. Hence the local pressure and force on the sea bed will be changed. $U_a(y)$ in Eq. 17 is set to 0.5m/s and wave period T is 3s. The generated wave height H_0 is about 0.4m and wave length is 10m. One fact needed to be pointed out is that the wave simulated in this paper is not so strong that the excessive pore water pressure can't cause dramatic change in liquefaction zone. But the main purpose of this paper is to demonstrate the new methodology of coupled solver of free surface fluid field and Biot consolidation equations. In order to simulate real storm waves, more computation resource is needed. Future research can use parallel

computation to decrease the computational time and simulate bigger domain with higher wave height.

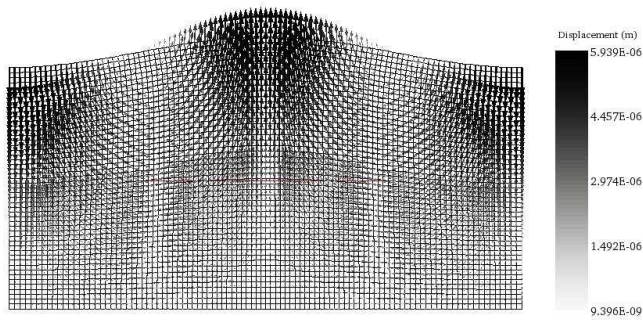


Fig. 7 Displacement Vector Field (Geometry Distorted)

Fig. 8 shows the fluid force components and magnitude on the object. The forces on the object undergo periodical changes. The most significant components are in the streamwise direction and vertical direction which is as expected. The spanwise fluid force is very small comparing with the other two. Second mode effect can also be seen in the figure but is not significant. This could be caused by the wave reflection from the object or the wave tank end. The forces are used to calculate the traction boundary condition on the object bottom.

In Fig. 9, the free surface of waves in one typical period is plotted. The blockage effect of the object in the wave tank modified the wave around it. The wave height relative to the water depth can also be seen.

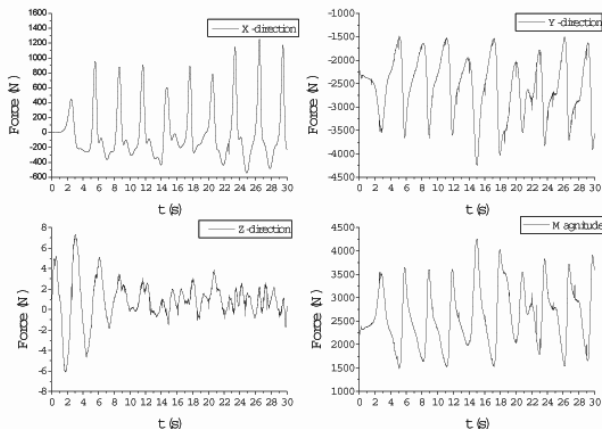


Fig. 8 Object Force History

Fig. 10 shows the iso-surface of the dimensionless instantaneous excessive pore pressure inside the sea bed. With the propagation of the wave, the sea bed pressure response also moves forward accordingly.

Fig. 11 is the contour plot of non-dimensionalized excessive pore pressure under the instantaneous flow field ($t = t_0 + \frac{3T}{4}$) in Fig. 9. The reason to plot for this time point is that the wave crest is almost on

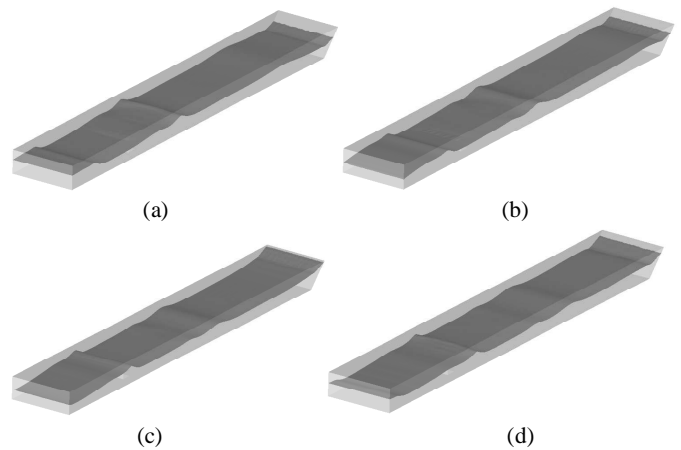


Fig. 9 Free Surface of Waves in One Typical Period: (a) $t=t_0+\frac{T}{4}$ (b) $t=t_0+\frac{T}{2}$ (c) $t=t_0+\frac{3T}{4}$ (d) $t=t_0+T$

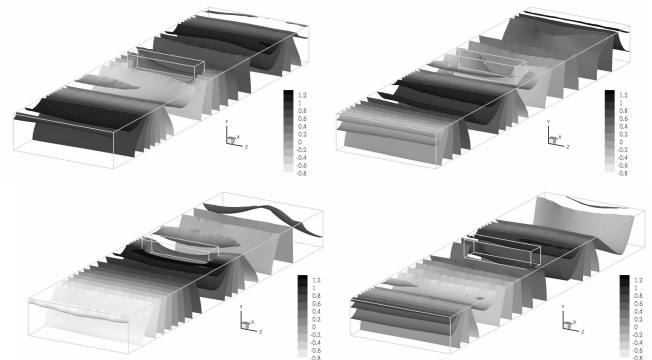


Fig. 10 Dimensionless Excessive Pore Pressure under Waves in One Typical Period: (a) $t = t_0 + \frac{T}{4}$ (b) $t = t_0 + \frac{T}{2}$ (c) $t = t_0 + \frac{3T}{4}$ (d) $t = t_0 + T$

the top of the object and it's considered to be the most possible time for the momentary liquefaction to happen. From the figures, it's clear the pressure distribution is disturbed by the half buried object. At this very moment, the excessive pore pressure in front of the object is very high and the liquefaction potential in this area and under the object is amplified. From the slice view, the excessive pore pressure beneath the object is also at the peak value. This is caused by two facts. One is that the wave crest is just above the object. The other is that the fluid forces on the object are also at maximum values.

DISCUSSION

Soil Constitutive Model Effects

For geotechnical problems, a realistic stress-strain constitutive relationship is one of the most important things for the ability of the numerical model to reproduce the reality situations. In this paper, the simple linear isotropic elastic model is used to describe the soil skeleton. More advanced and accurate constitutive models (such as

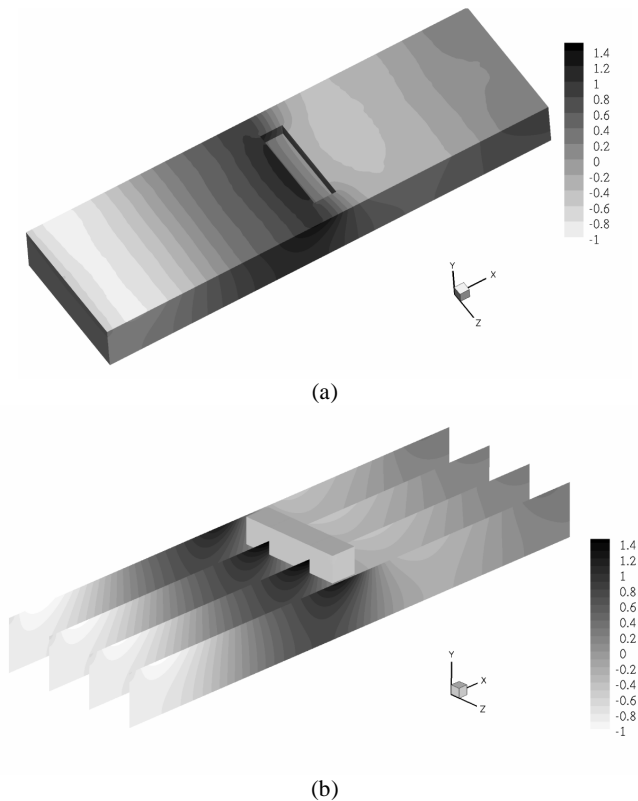


Fig. 11 Dimensionless Excessive Pore Pressure on the Bottom Corresponding to the Moment of Fig. 9: (a) 3D view of the Bottom Pressure (b) Slice View of the Bottom Pressure

variable elasticity, elastoplastic model and viscoplastic model, etc.) can be easily incorporated in the current numerical code. Anisotropic effect can also easily come into the model since the code is based on the tensorial description of the equations and anisotropic tensors can be included inside the differential operators.

Residual Liquefaction Effects

Only momentary liquefaction is model in this paper since it's simple and easy. Liquefaction is an complicated physical process which is still not well understood today. Liquefaction is generally caused by two main mechanisms: momentary liquefaction and residual liquefaction (Sumer and Fredsøe, 2002). Residual liquefaction is more complicated than momentary liquefaction because the pore pressure builds up with time. Some simplified models existing for the residual liquefaction add a source term to the governing equation of pore pressure. This can also easily be incorporated into current model. Further research is needed to carefully verify the parameters and to what happens after the liquefaction.

Bed Morphodynamics and Object Movement

In the wave-seabed-object system, another process, sediment transport, is also very important and is closely related the flow field and bed soil. Flow field change around the object causes scour and deposition of the sediment. Sediment movement will change the sea bed elevation and consequently affect the flow field. This sea bed change also will change the domain of the consolidation and change the pore pressure distribution. Scour is one of the main reasons of foundation failure in ocean and river engineering. Sediment transport together with the other

processes modeled in this paper forms an even bigger coupled system. Sediment transport and morphodynamic models should be included in the future.

The object is assumed to be at fixed position during the computation. This is not always true since when the liquefaction occurs, the soil can't support the object any more and the object will move. Even without liquefaction, the object could rotate or slide under the influence of fluid force. All these make the problem extremely complicated and it's impossible to include all factors into the numerical model. But by fixing the object in one position, it is possible to investigate the possibility of liquefaction and analyze the dynamics of the system. This could be useful for engineers to design structure and foundations to prevent damage under extreme conditions.

CONCLUSIONS

The numerical model in this paper can solve the coupling problem between waves, object (structure) and sea bed response. Sea bed response under wave is one of the keys to the understanding of liquefaction. The wave induced shear stress and pore pressure in the soil is governed by Biot consolidation equation. Free surface is modeled by Volume of Fluid (VOF) method and water wave is generated by numerical wave maker boundary condition. Instead of using finite element method to do stress analysis inside the bed material which is the traditional method used in geotechnics, an iterative numerical scheme is proposed to solve Biot consolidation equation using finite volume method. The new scheme shows fast convergence rate and high accuracy. The coupling between water wave and sea bed is through pressure and stress condition on common boundaries. Two numerical tests of the proposed scheme are carried out. First numerical case tests the consolidation solver part of the numerical model. Good agreement with analytical results is obtained. The second case is a 3D test to study the interaction between wave, sea bed and object. A box is half buried in the wave tank. More complicated real geometry can be simulated as well. From the result excessive pore pressure of the sea bed, liquefaction potential can be analyzed. Only momentary liquefaction can be studied using current model. For residual liquefaction, the modified Biot consolidation equation should be solved. The model proposed in this paper can be used to guide the design of under water structures and foundations.

ACKNOWLEDGEMENTS

The support from the coastal Geoscience Program of the U.S. Office of Naval Research (Grant N00014-05-1-0083) is gratefully acknowledged.

REFERENCES

- Aliabadi, S, Abedi, J, Zellars, B, Bota, K and Johnson, A (2003). "Simulation Technique For Wave Generation," *Communications in Numerical Methods in Engineering*, Vol 19, pp 349-359.
- Biot, M (1941). "General Theory of Three-dimensional Consolidation," *Journal of Applied Physics*, Vol 12, No 2, pp 154-164.
- Demidžić, I, Muzaferija, S and Perić, M (1994). "Finite Volume Method for Stress Analysis in Complex Domains," *International Journal For Numerical Methods In Engineering*, Vol 37, pp 3751-3766.
- Demidžić, I, Muzaferija, S and Perić, M (1997). "Benchmark Solutions of Some Structural Analysis Problems Using Finite-volume Method and Multigrid Acceleration," *International Journal For Numerical Methods In Engineering*, Vol 40, pp 1893-1908.
- Gao, F, Jeng, D and Sekiguchi, H (2003). "Numerical Study on the Interaction Between Non-linear Wave, Buried Pipeline and Non-homogeneous Porous Seabed," *Computers and Geotechnics*, Vol 30,

- pp 47-73.
- Issa, R (1986). "Solution of the Implicitly Discretised Fluid Flow Equations by Operator-splitting," *Journal of Computational Physics*, Vol 62, No 1, pp 40-65.
- Jasak, H (1996). "Error Analysis and Estimation for the Finite Volume Method with Application to Fluid Flows," *PhD thesis*, Imperial College of Science, Technology and Medicine, UK.
- Jasak, H, and Weller, H (2000). "Application of the Finite Volume Method and Unstructured Meshes to Linear Elasticity," *International Journal of Numerical Methods in Engineering*, Vol 48, pp 267-287.
- Jeng, D and Hsu, J (1996). "Wave-induced Soil Response in a Nearly Saturated Seabed of Finite Thickness," *Géotechnique*, Vol 46, No 3, pp 427-440.
- Jeng, D, and Lin, Y (1999). "Wave-induced Pore Pressure Around a Buried Pipeline in Gibson Soil: Finite Element Analysis," *International Journal of Numerical and Analytical Methods in Geomechanics*, Vol 23, No 13, pp 1559-1578.
- Lauder, B and Spalding D (1973). "The Numerical Computation of Turbulent Flows," *Computer Methods in Applied Mechanics and Engineering*, Vol 3, No 2, pp 269-289.
- Lewis, R and Schrefler, B (1998). "The Finite Element Method in the Static and Dynamic Deformation and Consolidation of Porous Media," John Wiley & Sons, second edition.
- Magada, W (1996). "Wave-induced Uplift Force Acting on a Submarine Buried Pipeline: Finite Element Formulation and Verification of Computations," *Computers and Geotechnics*, Vol 19, No 1, pp 47-73.
- Mayer, S and Garapon, A and Sorensen, L (1998). "A Fractional Step Method for Unsteady Free-surface Flow with Application to Non-linear Wave Dynamics," *International Journal for Numerical Methods in Fluids*, Vol 28, pp 293-315.
- Mei, C and Foda, M (1981). "Wave-induced Response in a Fluid-filled Poro-elastic Solid With a Free Surface-a Boundary Layer Theory," *Geophys. J. Roy. Astron. Soc.*, Vol 66, pp 597-631.
- OpenFOAM (2005). <http://www.openfoam.org>.
- Patank, S (1981). "Numerical Heat Transfer and Fluid Flow," McGraw-Hill.
- Sakai, T, Gotoh, H and Yamamoto, T (1994). "Block Subsidence Under Pressure and Flow," *Proc 24th Conference on Coastal Engineering (ICCE94)*, Kobe, Japan, pp 23-28.
- Sumer, B.M., Fredsøe, J, Christensen, S and Lind, M (1999). "Sinking/Floatation of Pipelines and Other Objects in Liquefied Soil Under Waves," *Coastal Engineering*, Vol 38, No 1, pp 53-90.
- Sumer, B.M., and Fredsøe, J (2002). "The Mechanics of Scour in the Marine Environment," World Scientific Publishing, New Jersey, USA.
- Ubbink, O and Issa, R (1999). "A Method for Capturing Sharp Fluid Interfaces on Arbitrary Meshes," *Journal of Computational Physics*, Vol 153, pp 26-50.
- Weller, H, Tabor, G, Jasak, H and Fureby, C (1998). "A Tensorial Approach to Computational Continuum Mechanics Using Object-oriented Techniques," *Computer in Physics*, Vol 12, No 6, pp 620-631.
- Yamamoto, T (1977). "Wave-induced Instability in Seabed," *Proc. ASCE Special Conference, Coastal Sediments '77*, Charleston, SC, pp 898-913.
- Yuhi, M and Ishida, H (2002). "Simplified Solutions for Wave-induced Response of Anisotropic Seabed," *Journal of Waterway, Port, Coastal and Ocean Engineering*, Vol 18, No 1, pp 46-50.